ACS Catalysis

pubs.acs.org/acscatalysis Letter

Decoding the Cytochrome P450 Catalytic Activity in Divergence of Benzophenone and Xanthone Biosynthetic Pathways

Ya Wang, Ana Luisa Malaco Morotti, Yiren Xiao, Zhuo Wang, Song Wu, Jianghua Chen, and Evangelos C. Tatsis*

Cite This: *ACS Catal.* 2022, 12, 13630−13637 Read Online

ACCESS | Metrics & More | Article Recommendations | Supporting Information

ABSTRACT: Plant benzophenones and xanthones have an impressive spectrum of biological activities. Here, we characterized three cytochrome P450 (CYP) enzymes from the *Garcinia xanthochymus* tree that convey 2,4,6-trihydroxybenzophenone (2,4,6-triHB) toward the diversification between the biosynthesis of benzophenones and xanthones. The CYP3 catalyzes the transformation of 2,4,6-triHB to 2,3′,4,4′,6-pentahydroxybenzophenone (2,3′,4,4′,6-pentaHB) through two consecutive hydroxylations, while the paralog CYP1 catalyzes the synthesis of 1,3,7-trihydroxyxanthone (1,3,7-triHX). To understand the product diversity, we performed homology modeling and active site-directed reciprocal mutations on CYP3. The mutant enzyme assays revealed the key role of the V375 residue. Although the V375A mutation favors the 1,3,7-triHX formation, the V375L enhances further the yield of 2,3′,4,4′,6-pentaHB. The engineered triple mutant CYP3-V375L/S479A/K480H demonstrated an improved product specificity and catalytic transformation toward 2,3′,4,4′,6-pentaHB. Our results represent an advance in the metabolism of benzophenones and xanthones, laying the foundation for discovery of downstream genes and even the production of new derivatives. The engineering of CYP enzymes that stand in divergence of biosynthetic pathways for benzophenones and xanthones provides the basis for designing new drugs and facilitates future synthetic biology applications.

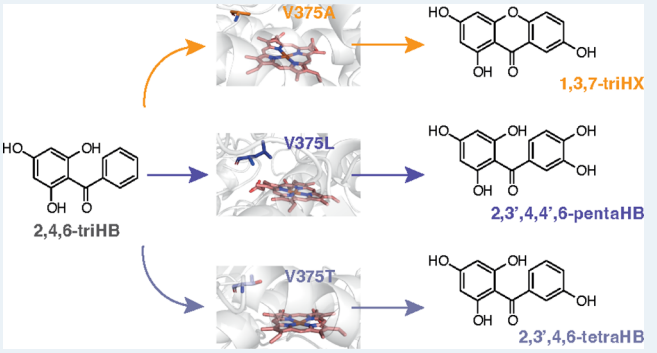

KEYWORDS: *biosynthesis, plant natural products, cytochrome P450, benzophenone, xanthone*

Benzophenones and xanthones are two classes of polyphenolic compounds with a $C_6-C_1-C_6$ carbon skeleton, which are extensively used for industrial[1] and medicinal applications,[2,3] mainly due to their photophysical properties. In nature, benzophenones and xanthones are widespread among bacteria,[4] fungi,[4,5] and plants,[5,6] with the dominant majority (∼80%) of compounds from the two classes mainly isolated from plants of Clusiaceae, Hypericaceae, Calophyllaceae, and Gentianaceae families.[5,6] Benzophenones and xanthones are abundant in the edible fruits from Garcinia genus (Clusiaceae) trees. In South East Asia, the consumption of fruits from *Garcinia xanthochymus*[7] and *Garcinia mangostana* (nicknamed as the queen of fruits),[8] is considered beneficial for human health. Benzophenones from Garcinia plants like garcinol and oblongifolin A[9,10] and xanthones such as gambogic acid and α-mangostin[11,12] (Figure 1) have been proposed as probes for development of novel anticancer drugs as these compounds are effective inhibitors of various key signaling pathways in cancer cells, such as NF-kB[13] and STAT3,[14] and induce apoptosis.[15] The structural diversity of bioactive natural benzophenones and xanthones have stimulated the chemical synthesis and biosynthetic studies.[2,4−6,16−18] In both plants and fungi, benzophenones and xanthones have precursor−product relationships, and their biosynthetic pathways (Figure S1) have evolved by convergence.[19,20] In plants, benzophenone synthase (BPS),[19] a plant type III polyketide synthase, catalyzes the synthesis of 2,4,6-trihydroxybenzophenone (2,4,6-triHB), while cytochrome P450 enzymes catalyze the transformation of 2,4,6-triHB to 1,3,7-trihydroxyxanthone (1,3,7-triHX) or 1,3,5-trihydroxyxanthone (1,3,5-triHX)[20] (Figure 1, Figure S1). The benzophenone and xanthone scaffolds can be further functionalized by introducing hydroxy groups in aromatic multiple positions; however, the enzymes involved were unknown until the present work.

Here, we investigate the cytochrome P450 enzymes, which catalyze the synthesis of highly oxidized 2,3′,4,4′,6-pentahy-

Received: July 15, 2022
Revised: September 29, 2022
Published: October 25, 2022

https://doi.org/10.1021/acscatal.2c03405
ACS Catal. 2022, 12, 13630−13637

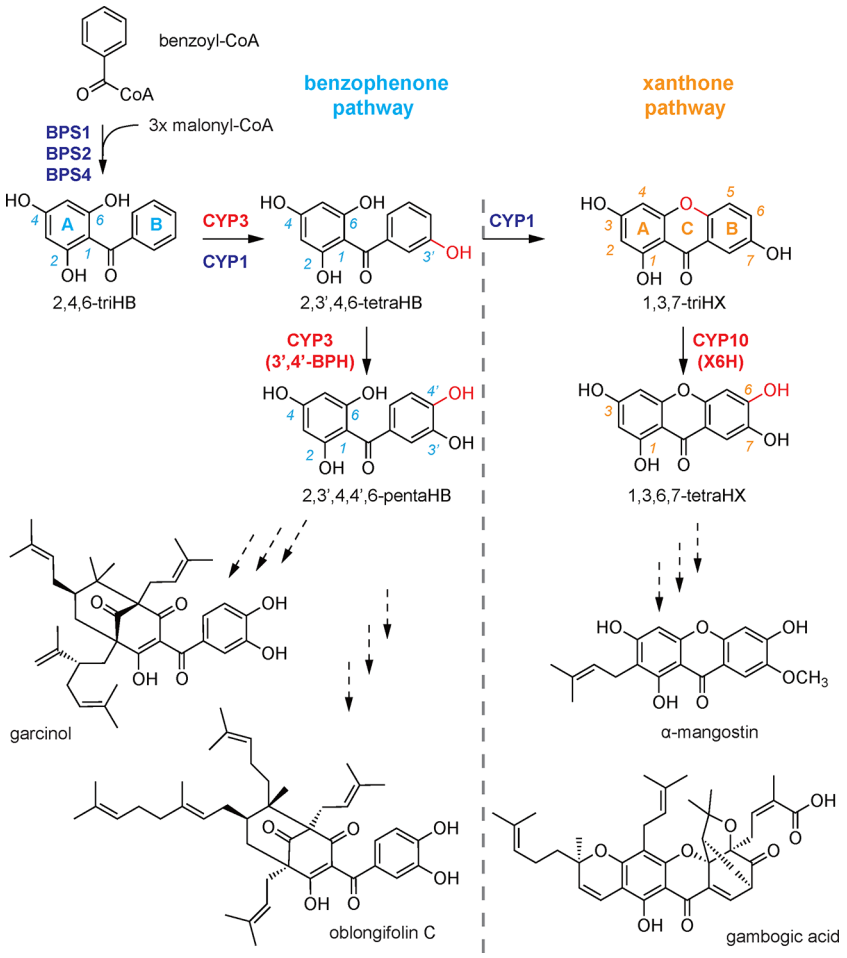

Figure 1. The benzophenone and xanthone metabolic pathways in *Garcinia* genus. Benzophenone synthase (BPS), a type III polyketide synthase, uses one benzoyl-CoA and three malonyl-CoA molecules to catalyze the formation of 2,4,6-trihydroxybenzophenone (2,4,6-triHB). Cytochrome P450 enzymes (CYPs) oxidize different carbons of 2,4,6-triHB ring B toward the formation of key precursors 2,3′,4,4′,6-pentahydroxybenzophenone (2,3′,4,4′,6-pentaHB) and 1,3,6,7-tetrahydroxyxanthone (1,3,6,7-tetraHX) in benzophenone and xanthone metabolic pathways, respectively. CYP1 initially catalyzes the hydroxylation on C(3′) of 2,4,6-triHB to yield 2,3′,4,6-tetrahydroxybenzophenone (2,3′,4,6-tetraHB) and at the second step the phenolic coupling oxidation between C(2)OH and C(6) of 2,3′,4,6-tetraHB to give the 1,3,7-trihydroxyxanthone (1,3,7-triHX). CYP3 transforms the 2,4,6-triHB to 2,3′,4,4′,6-pentaHB through 2,3′,4,6-tetraHB. CYP10 acts as xanthone-6-hydroxylase on 1,3,7-triHX. The enzymes characterized in the current study are highlighted in red.

droxybenzophenone (2,3′,4,4′,6-pentaHB) and 1,3,6,7-tetrahydroxyxanthone (1,3,6,7-tetraHX). Both 2,3′,4,4′,6-pentaHB and 1,3,6,7-tetraHX are key precursors in biosynthetic pathways for most of the medicinally important benzophenones and xanthones, such as garcinol and α-mangostin, respectively (Figure 1). Furthermore, based on homology modeling, active site mutations and functional evaluation of mutant enzymes, we identified a single amino acid residue that controls the diversification of benzophenones and xanthones biosynthesis.

In this study, we established metabolomic (Figure S2) and transcriptomic data (Figure S3, Table S1, S2) for several plant tissues collected from *G. xanthochymus* trees. We chose four candidate BPS genes from *G. xanthochymus* transcriptomic data based on sequence similarity with characterized GmBPS.[19] Candidate BPS enzymes were expressed (Figure S4) and assayed with benzoyl-CoA and malonyl-CoA as substrates. The 2,4,6-triHB was the predominant enzymatic product for BPS1, BPS2, and BPS4, while BPS3 showed no activity under the tested conditions (Figure S4). Determination of steady-state kinetics (Table S3) shows that BPS1 has the highest affinity for benzoyl-CoA with a K_m of 14.26 μM, with a k_{cat}/K_m ratio 0.33 $s^{-1}\cdot\mu M^{-1}$ comparable to GmBPS (0.34 $s^{-1}.\mu M^{-1}$). Enzymatic transformations of 2,4,6-triHB into key precursors 2,3′,4,4′,6-pentaHB and 1,3,6,7-tetraHX require several oxidation steps at multiple positions (Figure 1), and therefore, we focused on cytochrome P450 enzymes.

To search for cytochrome P450s, we organized the transcriptomic data based on the gene expression profile across different tissues in clusters (nodes) using a self-organizing map (SOM; Figure S5).[21−23] Then we focused on (i) candidate genes placed within or adjacent to nodes containing any of enzymatically active BPS genes in SOM and (ii) candidate genes with expression profile correlated with accumulation of 2,3′,4,4′,6-pentaHB, garcinol, 1,3,6,7-tetraHX, and α-mangostin. Our metabolomic data show that xanthones are found in high levels in sepals and fruit pedicel, while benzophenones are accumulated at high levels in fruit tissues (pulp, pericarp, pedicel) and sepals (Figure S2). The highest expression for *BPS1* and *BPS2* genes was observed in similar tissues like sepal and fruit pedicel (Figure S6). Nine putative P450 genes from different CYP families (Table S4) were

https://doi.org/10.1021/acscatal.2c03405
ACS Catal. 2022, 12, 13630−13637

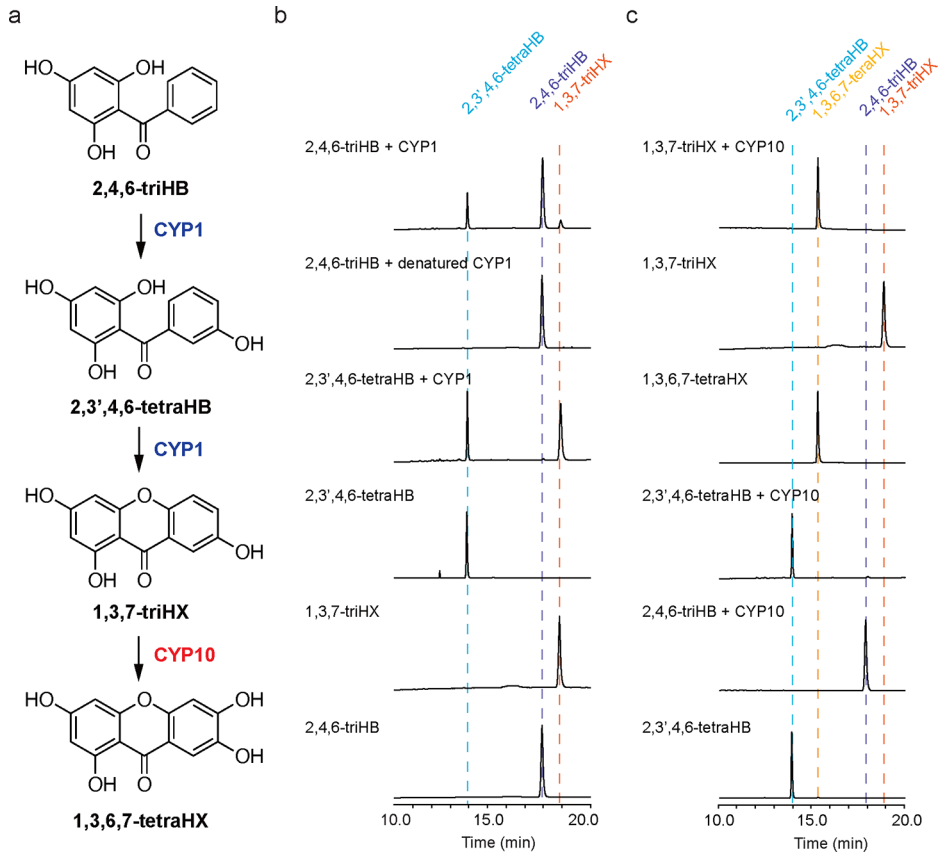

Figure 2. Characterization of *Garcinia xanthochymus* cytochrome P450 enzymes activities in 1,3,6,7-tetrahydroxyxanthone (1,3,6,7-tetraHX) biosynthesis. (a) The pathway from 2,4,6-triHB to 1,3,6,7-tetraHX. (b) HPLC-DAD chromatographic profile at 306 nm of different benzophenone, xanthone analytical standards, and CYP1 enzyme assays on 2,4,6-triHB. Denatured (boiled) CYP1 was used as the negative control. (c) HPLC-DAD chromatographic profile at 315 nm of different benzophenone, xanthone analytical standards, and CYP10 enzyme assays on 2,4,6-triHB, 2,3′,4,6-triHB, and 1,3,7-triHX.

selected for functional characterization supported by mining and correlation of transcriptomic and metabolomic data.

We cloned the CYP genes ORF into expression vectors (pESC-Leu), and we expressed these enzymes in yeast (WAT11 cells)[24] (Figure S7). Microsomes harboring P450 enzymes were assayed against synthesized 2,4,6-triHB (100 μM) in the presence of NADPH (500 μM), and results were analyzed by HPLC coupled with DAD and LCMS. For the rapid identification of potential products, we established a library of benzophenone and xanthone compounds (Table S5, Schemes S1−S3) that may be products or byproducts of 2,4,6-triHB oxidations. These standards were used to establish calibration curves for quantification of enzymatic products by LC-tQ-MS (Figure S8−S9). No enzymatic products were detected in assays that either lacked NADPH or contained microsomes from yeast harboring the empty plasmid. Microsomal fractions harboring P450 enzymes that failed to show any enzyme activity were not studied further.

The CYP1 enzyme assays showed the formation of two new products; the product eluted at 13.9 min with UV peaks at 259 and 306 nm and with (MS/MS) spectra fragments at m/z 245.05, 151.00, 107.01, and it was identified as 2,3′,4,6-tetraHB based on comparison with standard (Figure 2, Figure S10). Likewise, the CYP1 enzyme assay product eluted at 18.8 min with UV peaks at 256, 236, and 310 nm and (MS/MS) spectra fragments at m/z 243.03, 199.04, and 143.05, and it was identified as 1,3,7-triHX after comparison with standard (Figure 2, Figure S10). Quantification by LC-tQ-MS of the CYP1 enzyme assays with 2,4,6-triHB showed the release of 40.80% 2,3′,4,6-tetraHB, 54.90% 1,3,7-triHX and 4.30% 2,3′,4,4′,6-pentaHB as products (Table S6). When the CYP1 was assayed with 2,3′,4,6-tetraHB as substrate, resulted to 93.25% 1,3,7-triHX and 6.75% 2,3′,4,4′,6-pentaHB as products (Table S7). Thus, we concluded that CYP1 acts as benzophenone 3′-hydroxylase (B3′H) and 1,3,7-trihydroxyxanthone synthase (1,3,7-TXS).

The CYP10 was annotated as cytochrome CYP71A9 with 53% sequence identity to isoflavone 2′-hydroxylase from *Glycine max* (Table S4),[25] it did not show enzymatic activity toward 2,4,6-triHB or 2,3′,4,6-tetraHB, but when CYP10 was assayed with 1,3,7-triHX, a new product eluted at 15.3 min, with UV peaks at 254, 237, and 315 nm and MS/MS fragments at m/z 259.02 and 215.03 (Figure 2, Figure S11). The CYP10 product was identified as 1,3,6,7-tetraHX since the chromatographic (Rt) and spectral data (UV, MS, MS^2) matched with the authentic standard (Figure S11). Therefore, the CYP10 is functionally characterized as xanthone-6-hydroxylase (X6H). Although X6H activities have been described in the cell cultures of *Hypericum androsaemum* and *Centaurium erythraea*,[26] CYP10 as reported here is the first enzyme with X6H activity. Since the CYP10 (X6H) enzymatic product 1,3,6,7-tetraHX scaffold is the most abundant among xanthone derivatives in the plant kingdom, the discovery of a gene with X6H activity opens new gateways for future gene discovery in

https://doi.org/10.1021/acscatal.2c03405
ACS Catal. 2022, 12, 13630−13637

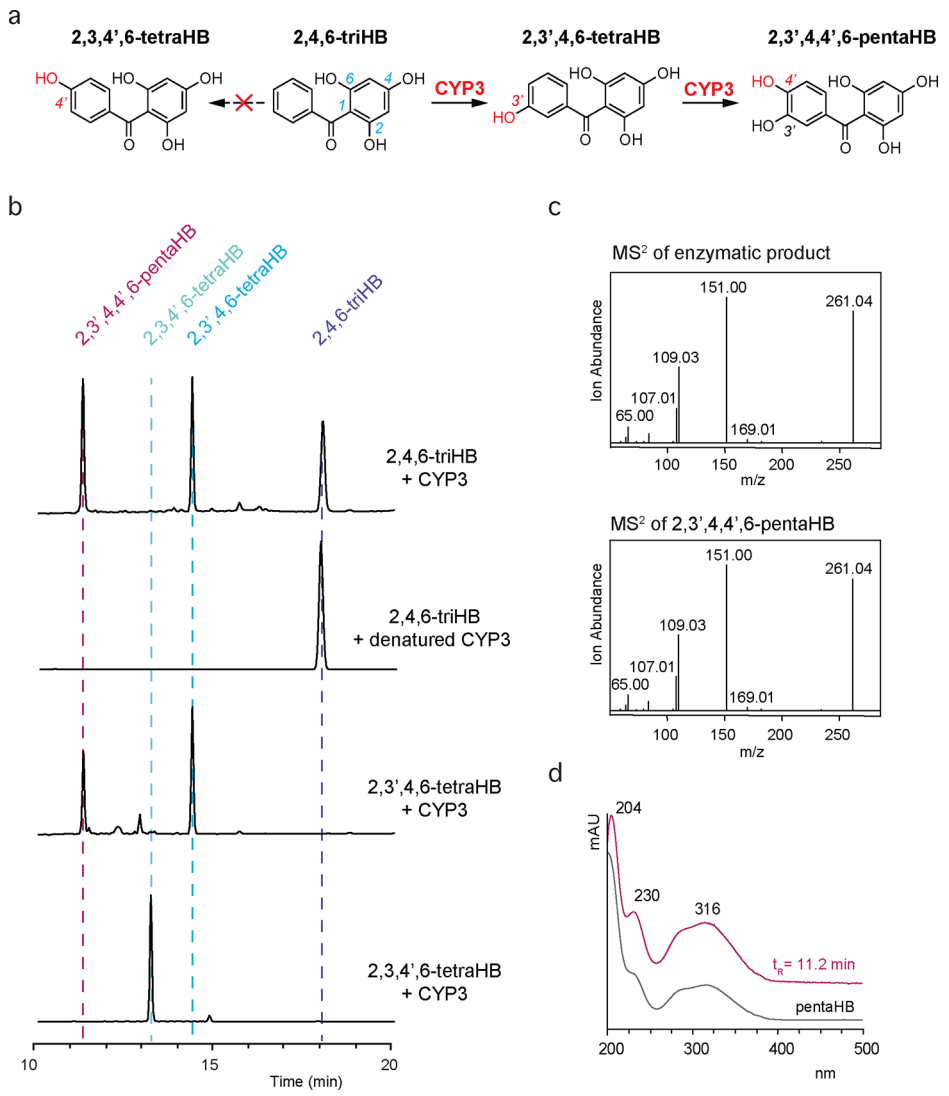

Figure 3. Characterization of *Garcinia xanthochymus* cytochrome P450 CYP3 enzyme activities in 2,3′,4,4′,6-pentahydroxybenzopheone (2,3′,4,4′,6-pentaHB) biosynthesis. (a) The pathway from 2,4,6-triHB to 2,3′,4,4′,6-pentaHB proceeds through 2,3′,4,6-tetraHB and not through 2,4,4′,6-tetraHB. (b) HPLC-DAD chromatographic profile at 315 nm of CYP3 enzyme assays on 2,4,6-triHB, 2,3′,4,6-triHB and 2,4,4′,6-tetraHB. Enzyme assays with denatured (boiled) CYP3 was used as negative control. The identity of eluted metabolites was confirmed by comparison with authentic standards. (c) Comparison of MS^2 spectra of 2,3′,4,4′,6-pentaHB synthetic standard and coeluted CYP3 enzymatic product with major peaks at *m*/*z* 151.00, 261.04, 109.03, and 107.01. (d) Comparison of UV−vis spectra of CYP3 enzymatic product eluted at 11.2 min (highlighted in magenta color) and of 2,3′,4,4′,6-pentaHB synthetic standard, with maxima at 204, 230, and 316 nm.

xanthone metabolism, enabling synthetic biology and metabolic engineering applications for the heterologous production of economic important xanthones (Figure S12).

Incubation of microsomes expressing CYP3 with 2,4,6-triHB and NADPH led to the formation of two products as the enzyme analyzed by HPLC; the first product is eluted at 11.2 min with UV peaks at 230 and 316 nm, and the second one is eluted at 14.3 min with UV peaks at 259 and 306 nm, respectively (Figure 3, Figure S13). Based on comparison with retention time, UV, MS, and MS^2 spectra of authentic standards, the product eluted at 14.3 min was identified as 2,3′,4,6-tetraHB, and the product eluted at 11.2 min was identified as 2,3′,4,4′,6-pentaHB (Figure 3, Figure S13). To check the sequential order of hydroxylation steps catalyzed by CYP3, and determine if hydroxylation on C(3′) of 2,4,6-triHB occurs first, and the hydroxylation on C(4′) follows or the reverse order, we used the two tetrahydroxy benzophenone isomers, 2,3′,4,6-tetraHB and 2,4,4′,6-tetraHB, as substrates and incubated with CYP3 microsomes. No enzymatic activity was observed by CYP3 with 2,3,4′,6-tetraHB as the substrate, whereas when CYP3 was incubated with 2,3′,4,6-tetraHB, the formation of 2,3′,4,4′,6-pentaHB as major product was observed (Figure 3, Figure S13, Table S7). Quantification of CYP3 enzymatic products with 2,4,6-triHB as the substrate showed release of 64.67% 2,3′,4,6-tetraHB, 2.48% 1,3,7-triHX, and 32.85% 2,3′,4,4′,6-pentaHB (Figure 4a, Table S6). However, the quantification of CYP3 enzyme assays with 2,3′,4,6-tetraHB as the substrate revealed 98.90% of 2,3′,4,4′,6-pentaHB and 1.10% of 1,3,7-triHX as products (Figure 4a, Table S7). These results show that CYP3 catalyzes first the hydroxylation at C(3′) and the biosynthesis of penta-HB proceeds through 2,3′4,6-tetraHB. In consequence, CYP3 was identified as a bifunctional enzyme, catalyzing two tandem hydroxylations at C(3′) and C(4′) of 2,4,6-triHB toward formation of 2,3′,4,4′,6-pentaHB. Since the majority of PPAPs in Garcinia species are derived from 2,3′,4,4′,6-pentaHB, the

https://doi.org/10.1021/acscatal.2c03405
ACS Catal. 2022, 12, 13630−13637

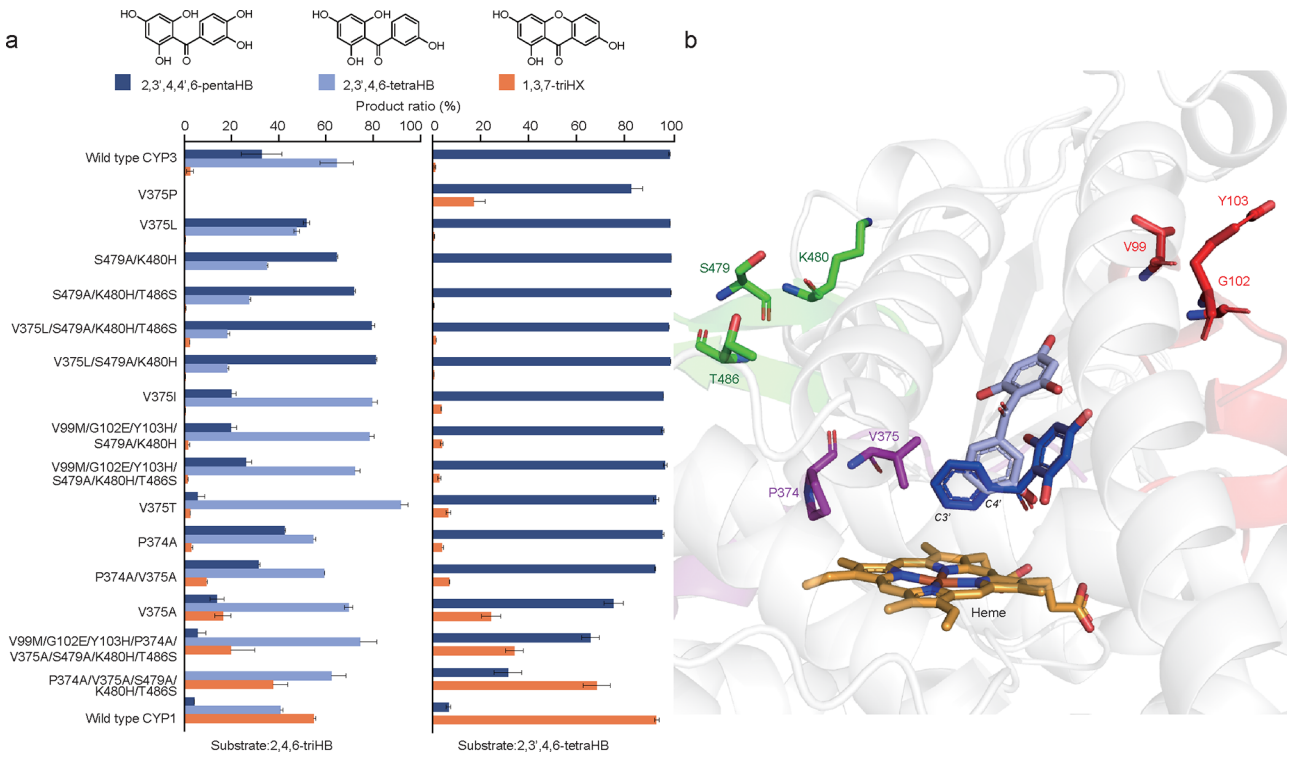

Figure 4. Engineering the CYP3 to improve the 2,3′,4,4′,6-pentahydroxybenzophenone synthesis. (a) Product profiles of wild-type CYP3 and CYP3 mutant enzymes with 2,4,6-triHB and 2,3′,4,6-tetraHB as substrates based on quantification by LC-tQMS. The light blue bars represent the 2,3′,4,6-tetraHB product ratio (%), the dark blue bars represent the 2,3′,4,4′,6-pentaHB product ratio (%), and orange bars represent the 1,3,7-triHX product ratio (%). Data bars represent s.d. for three replicates. (b) Superimposed docking results of substrates 2,4,6-triHB (dark blue) and 2,3′,4,6-tetraHB (light blue) in the model structure of CYP3. Amino acid residues selected as targets for site-directed mutagenesis are highlighted in red (SRS1), purple (SRS5) and green (SRS6) sticks. Heme is highlighted in orange color. The rest of the enzyme is depicted in gray.

discovery of CYP3 is an essential milestone to harness the diversity of a large family of bioactive compounds with a broad plethora of medicinal activities.

Both CYP1 and CYP3 catalyze the first hydroxylation on C(3′) for synthesis of 2,3′,4,6-tetraHB with CYP1 showing increased affinity toward 2,4,6-triHB (CYP1 K_m = 0.51 μM; Table S10) compared with CYP3 (CYP3 K_m = 38.39 μM; Table S10). CYP1 catalyzes mainly the oxidative phenol coupling of 2,3′,4,6-tetraHB for synthesis of 1,3,7-triHX (CYP1 K_m = 2.22 μM; Table S10), and CYP3 catalyzes mainly the second hydroxylation of 2,3′,4,6-tetraHB on C(4′) for synthesis of 2,3′,4,4′,6-pentaHB (CYP3 K_m = 8.14 μM; Table S10). The functions of CYP1 and CYP3 as biocatalysts highlight the entry into different chemical space and play significant role in bifurcation between the metabolic pathways of benzophenones and xanthones (Figure 1). These two biocatalysts demonstrate a dramatically different product profile with mixture between 2,3′,4,6-tetraHB, 2,3′,4,4′,6-pentaHB and 1,3,7-triHX (Figure 4a, Tables S6−S9), although they share high (≈ 80%) sequence similarity (Figure S14), providing the molecular basis to understand the generation of stereochemical diversity.

We took advantage of different protein structure prediction tools such as MODELER,[27] I-TASSER,[28] Phyre2,[29] and AlphaFold2[30] to construct model protein structures of CYP1 and CYP3 (Figures S15, S16) and identify the major structural features (Figures S17, S18). CYP1 and CYP3 accept as substrates both 2,4,6-triHB and 2,3′,4,6-tetraHB, and thus, we focused on candidate mutations on the proximal side of active site, adjacent to the heme cofactor. To identify residues that may play a role in the outcome of oxidative reactions, we performed molecular docking using Autodock Vina[31] with the model structures of CYP3 generated by I-TASSER with the two substrates 2,4,6-triHB and 2,3′,4,6-tetraHB (Figure S19). We identified eight divergent amino acid residues located close to heme and point with their side chains toward the bound substrate (Figure S20). These eight divergent amino acid residues are parts of substrate-recognition sites (SRSs) SRS1, SRS5, SRS6 (Figure 4). The SRSs are considered common features among CYPs, and they are regarded to have a role in substrate binding and catalytic activity.[32−35] We performed reciprocal site-directed mutagenesis of the eight amino acid residues on CYP3 (Figure S20), and the enzymatic assay activity of the mutant enzymes was quantified by LC-tQMS for functional validation.

The enzyme assays of CYP3 octuple mutant showed an increase of 1,3,7-triHX formation ratio, to 19.78% with 2,4,6-triHB as substrate and 34.16% with 2,3′4,6-tetraHB, compared with wild type's (WT) 2.48% and 1.1%, respectively (Figure 4, Figure S21, Tables S6). Recombinant mutant enzymes CYP3-V99M/G102E/Y103H/S479A/K480H and CYP3-V99M/G102E/Y103H/S479A/K480H/T486S did not show any remarkable changes toward 1,3,7-triHX product ratio (Figure 4, Figure S21, Tables S6) while the enzyme assays of single and double mutants CYP3-P374A, CYP3-V375A, and CYP3-P374A/V375A with 2,4,6-triHB as substrate, revealed that the reciprocal mutation on amino acid residue V375A favors the formation of xanthone 1,3,7-triHX from 2.48% in WT to 16.40% for CYP3-V375A and 9.33% CYP3-P374A/V375A mutant enzymes. The enzyme assays of single mutant CYP3-

https://doi.org/10.1021/acscatal.2c03405
ACS Catal. 2022, 12, 13630−13637

V375A and the quintuple mutant CYP3-P374A/V375A/S479A/K480H/T486S showed the transformation of 2,3′4,6-tetraHB to 1,3,7-triHX at 24.4% and 60.4%, respectively, compared with 1.1% of WT, and practically switched the activity to 1,3,7-triHX synthesis. These data confirm the importance of 375 amino acid residue on controlling either the transformation of 2,3′4,6-tetraHB to 2,3′,4,4′,6-pentaHB or to 1,3,7-triHX (Figure 4, Figure S22, Tables S6, S7).

Valine is a branch chain amino acid with a bulkier hydrophobic side chain in comparison to alanine. To explore the role of the aliphatic hydrophobic side chain, we performed the following mutations V375T, V375L, V375I, and V375P and assayed them with 2,4,6-triHB and 2,3′,4,6-tetraHB. The more hydrophilic side chain of V375T mutation yielded the highest 2,3′,4,6-tetraHB percentage (91.79%) (Figure 4, Table S6) observed among all the mutants, suggesting that the presence of OH group may affect the interaction between the enzyme and 2,3′,4,6-tetraHB and prevent the second oxidation. The introduction of a longer amino acid side chain in V375L mutation resulted in a substantial increase of 2,3′,4,4′,6-pentaHB product ratio (51.84%) (Figure 4, Table S6). These results demonstrate that the size of an aliphatic side chain of amino acid 375 determines the outcome of biocatalysis either toward second tandem hydroxylation of benzophenone ring B (Figures 1, 3) or toward phenol coupling and formation of xanthone ring C (Figures 1, 2). It can be hypothesized that the aliphatic side chain of branch chain amino acids like valine or leucine affects the placement of the substrate in P450 active site by steric hindrance.

To rationalize our experimental findings on the biochemical activity of CYP3 mutants, we turned our attention to molecular modeling and docking data. In the docking model for 2,4,6-triHB into the homology model structure of wild-type CYP3, the substrate sits with the C(3′) over the active site of heme, while in the docking model for 2,3′,4,6-tetraHB, the configuration of the substrate in active site appears to be in different orientation, with the C(4′) of substrate pointing directly to the center of heme (Figure 4b, Figure S23). The mutation of V375A increases the available space in active site over heme and allows the free rotation of the 2,3′,4,6-tetraHB substrate, which favors the phenol coupling reactions leading to formation of 1,3,7-triHX as previously supported[20] (Figure S24a,b). In the docking model of the CYP3-V375L mutant, the presence of the L375 with the bulkier side chain affects the placement of the two substrates over the heme of P450 (Figure S24c-d). It can be hypothesized that the longer side chain of CYP3-V375L mutant in comparison to wild-type CYP3 V-375 reduces the space on active site and narrowing the possibility to catalyze the phenolic coupling reaction leading to formation of xanthone ring C (Figure 1).

Throughout the screening of enzymatic assays of mutant enzymes CYP3-S479A/K480H and CYP3-S479A/K480H/T486S, an unanticipated increase toward production of 2,3′,4,4′,6-pentaHB was observed at 64.52% and 71.85%, respectively (Figure 4a, Table S6). Although molecular docking did not reveal any interactions between the substrate and amino acids S479, K480, and T486, we suggest those amino acids play a role on substrate channelling and its orientation in the active site (Figure S19). To benefit from this serendipitous finding, we designed and expressed the chimeric proteins CYP3-V375L/S479A/K480H and CYP3-V375L/S479A/K480H/T486S to improve the transformation of 2,4,6-triHB toward 2,3′,4,4′,6-pentaHB. The enzyme assays of the two chimeric proteins showed the limited release of 1,3,7-triHX as product to 0.45% and 2.28% and the maximized the production of 2,3′,4,4′,6-pentaHB to 81.21% and 79.46%, respectively (Figure S25, Table S6).

Classical natural product chemistry works have implied the biogenetic relationships between xanthones and benzophenones,[5,6] however the metabolic crossroads between these two classes of natural products *in planta* were not fully understood. Here we characterized enzymes with new to literature activities of xanthone-6-hydroxylase (X6H) and benzophenone-3′,4′-hydroxylase (BP3′4′H) which catalyze the synthesis of central precursors 2,3′,4,4′,6-pentaHB in benzophenone pathway and 1,3,6,7-tetraHX in xanthone pathway. These newly identified genes can facilitate the future discovery of downstream genes in biosynthesis of important bioactive natural products such as garcinol, α-mangostin, and a plethora of natural benzophenones and xanthones, since knowing the metabolic steps and intermediates can assist to find the next biosynthetic steps (e.g., prenylransferases) through coexpression analysis of transcriptomic data.

Mining into native P450 promiscuity provides the opportunity to explain the pathway divergence between different scaffolds. *In silico* tools like molecular modeling, protein structure prediction, and molecular docking can assist to navigate toward the selection of amino acids that direct the enzymatic activities to different product profiles. Biochemical assays of mutant enzymes revealed the critical role of residue 375 side chain in CYP3 product divergence between xanthone and benzophenone. Further protein engineering provided chimeric enzymes with improved catalytic transformation toward the 2,3′,4,4′,6-pentaHB. These chimeric proteins can serve future synthetic biology and metabolic engineering applications to heterologous production of natural benzophenones and new to nature or rare benzophenones.

■ ASSOCIATED CONTENT

Data Availability Statement

Gene sequence data for this study have been deposited in the National Center for Biotechnology Information (NCBI) database: BPS1 ON989482; BPS2 ON989483; BPS4 ON989484; CYP1 (CYP81AA4) ON989485; CYP3 (CYP81AA5)ON989486; CYP10 (CYP71AH51) ON989487.

Supporting Information

The Supporting Information is available free of charge at https://pubs.acs.org/doi/10.1021/acscatal.2c03405.

Experimental procedures, supplementary tables S1−S11, supplementary schemes S1−S3, supplementary figures S1−S29, NMR spectra, HRMS and MS^2 data, references and author contributions (PDF)

■ AUTHOR INFORMATION

Corresponding Author

Evangelos C. Tatsis − *National Key Laboratory of Plant Molecular Genetics, CAS Center for Excellence in Molecular Plant Sciences, Shanghai 200032, China; CEPAMS - CAS-JIC Centre of Excellence for Plant and Microbial Sciences, Shanghai 20032, China;* orcid.org/0000-0002-4013-1537; Email: etatsis@cemps.ac.cn, evangelos.tatsis@jic.ac.uk

https://doi.org/10.1021/acscatal.2c03405
ACS Catal. 2022, 12, 13630−13637

Authors

Ya Wang − *National Key Laboratory of Plant Molecular Genetics, CAS Center for Excellence in Molecular Plant Sciences, Shanghai 200032, China; University of Chinese Academy of Sciences, Beijing 100049, China*

Ana Luisa Malaco Morotti − *National Key Laboratory of Plant Molecular Genetics, CAS Center for Excellence in Molecular Plant Sciences, Shanghai 200032, China*

Yiren Xiao − *National Key Laboratory of Plant Molecular Genetics, CAS Center for Excellence in Molecular Plant Sciences, Shanghai 200032, China; University of Chinese Academy of Sciences, Beijing 100049, China*

Zhuo Wang − *National Key Laboratory of Plant Molecular Genetics, CAS Center for Excellence in Molecular Plant Sciences, Shanghai 200032, China; University of Chinese Academy of Sciences, Beijing 100049, China*

Song Wu − *National Key Laboratory of Plant Molecular Genetics, CAS Center for Excellence in Molecular Plant Sciences, Shanghai 200032, China; University of Chinese Academy of Sciences, Beijing 100049, China*

Jianghua Chen − *CAS Key Laboratory of Tropical Plant Resources and Sustainable Use, Xishuangbanna Tropical Botanical Garden, Menglun 666303, China*

Complete contact information is available at: https://pubs.acs.org/10.1021/acscatal.2c03405

Notes

The authors declare no competing financial interest.

■ ACKNOWLEDGMENTS

We would like to acknowledge Prof. Xiao-Ya Chen (CEMPS) for the critical reading of the manuscript and for fruitful discussions. The authors would like to thank the CEMPS Core Facility Center for the excellent support in metabolomics and especially Mrs. Xiaoyan Xu, Mrs. Shanshan Wang, and Mr. Wenli Hu; and staff and administration of Xishuangbanna Tropical Botanical Garden (XTBG) for the access to *G. xanthochymus* plants. The work was financially supported by Strategic Priority Research Program of the Chinese Academy of Sciences grant XDB27020204; Chinese Academy of Sciences, International Partnership Program of CAS grant 153D31KYSB20160074; National Key Laboratory of Plant Molecular Genetics Special Fund. A.L.M.M. was awarded with CAS PIFI Fellowship and the China Postdoctoral Science Foundation for Postdoctoral International Exchange Program Fellowship.

■ REFERENCES

(1) Romero, N. A.; Nicewicz, D. A. Organic Photoredox Catalysis. *Chem. Rev.* **2016**, *116* (17), 10075−10166.

(2) Gunter, N. V.; Teh, S. S.; Lim, Y. M.; Mah, S. H. Natural Xanthones and Skin Inflammatory Diseases: Multitargeting Mechanisms of Action and Potential Application. *Front Pharmacol* **2020**, *11*, 594202.

(3) Dorman, G.; Prestwich, G. D. Benzophenone Photophores in Biochemistry. *Biochemistry* **1994**, *33* (19), 5661−5673.

(4) Masters, K.-S.; Bräse, S. Xanthones from Fungi, Lichens, and Bacteria: The Natural Products and Their Synthesis. *Chem. Rev.* **2012**, *112* (7), 3717−3776.

(5) Wu, S. B.; Long, C.; Kennelly, E. J. Structural diversity and bioactivities of natural benzophenones. *Nat. Prod Rep* **2014**, *31* (9), 1158−74.

(6) Remali, J.; Sahidin, I.; Aizat, W. M. Xanthone Biosynthetic Pathway in Plants: A Review. *Front Plant Sci.* **2022**, *13*, 809497.

(7) Wickramasinghe, P. C. K.; Murray, A. F.; Sahoo, M. R.; Dein, M.; Luckett, C. R.; Dia, V. P.; Munafo, J. P. The effects of processing on Garcinia xanthochymus fruit beverage. *Journal of Food Measurement and Characterization* **2020**, *14* (1), 55−68.

(8) Aizat, W. M.; Ahmad-Hashim, F. H.; Syed Jaafar, S. N. Valorization of mangosteen, "The Queen of Fruits," and new advances in postharvest and in food and engineering applications: A review. *J. Adv. Res.* **2019**, *20*, 61−70.

(9) Oike, T.; Ogiwara, H.; Torikai, K.; Nakano, T.; Yokota, J.; Kohno, T. Garcinol, a histone acetyltransferase inhibitor, radiosensitizes cancer cells by inhibiting non-homologous end joining. *Int. J. Radiat Oncol Biol. Phys.* **2012**, *84* (3), 815−21.

(10) Fuchs, R. A.; McLaughlin, R. J. Garcinol: A Magic Bullet of Amnesia for Maladaptive Memories? *Neuropsychopharmacology* **2017**, *42* (3), 581−583.

(11) Liu, Y.; Chen, Y.; Lin, L.; Li, H. Gambogic Acid as a Candidate for Cancer Therapy: A Review. *Int. J. Nanomedicine* **2020**, *15*, 10385−10399.

(12) Chi, Y.; Zhan, X. K.; Yu, H.; Xie, G. R.; Wang, Z. Z.; Xiao, W.; Wang, Y. G.; Xiong, F. X.; Hu, J. F.; Yang, L.; Cui, C. X.; Wang, J. W. An open-labeled, randomized, multicenter phase IIa study of gambogic acid injection for advanced malignant tumors. *Chin Med. J. (Engl)* **2013**, *126* (9), 1642−1646.

(13) Jia, Y.; Pang, C.; Zhao, K.; Jiang, J.; Zhang, T.; Peng, J.; Sun, P.; Qian, Y. Garcinol Suppresses IL-1β-Induced Chondrocyte Inflammation and Osteoarthritis via Inhibition of the NF-κB Signaling Pathway. *Inflammation* **2019**, *42* (5), 1754−1766.

(14) Sethi, G.; Chatterjee, S.; Rajendran, P.; Li, F.; Shanmugam, M. K.; Wong, K. F.; Kumar, A. P.; Senapati, P.; Behera, A. K.; Hui, K. M.; Basha, J.; Natesh, N.; Luk, J. M.; Kundu, T. K. Inhibition of STAT3 dimerization and acetylation by garcinol suppresses the growth of human hepatocellular carcinoma in vitro and in vivo. *Mol. Cancer* **2014**, *13*, 66.

(15) Mustachio, L. M.; Roszik, J.; Farria, A.; Dent, S. Y. R. Targeting the SAGA and ATAC Transcriptional Coactivator Complexes in MYC-Driven Cancers. *Cancer Res.* **2020**, *80* (10), 1905−1911.

(16) Kong, L.; Deng, Z.; You, D., Chemistry and biosynthesis of bacterial polycyclic xanthone natural products. *Nat. Prod Rep* **2022**. DOI: 10.1039/D2NP00046F

(17) Winter, D. K.; Sloman, D. L.; Porco, J. A., Jr. Polycyclic xanthone natural products: structure, biological activity and chemical synthesis. *Nat. Prod Rep* **2013**, *30* (3), 382−91.

(18) Yang, X. W.; Grossman, R. B.; Xu, G. Research Progress of Polycyclic Polyprenylated Acylphloroglucinols. *Chem. Rev.* **2018**, *118* (7), 3508−3558.

(19) Nualkaew, N.; Morita, H.; Shimokawa, Y.; Kinjo, K.; Kushiro, T.; De-Eknamkul, W.; Ebizuka, Y.; Abe, I. Benzophenone synthase from Garcinia mangostana L. pericarps. *Phytochemistry* **2012**, *77*, 60−69.

(20) El-Awaad, I.; Bocola, M.; Beuerle, T.; Liu, B.; Beerhues, L. Bifunctional CYP81AA proteins catalyse identical hydroxylations but alternative regioselective phenol couplings in plant xanthone biosynthesis. *Nat. Commun.* **2016**, *7*, 11472.

(21) Dang, T. T.; Franke, J.; Tatsis, E.; O'Connor, S. E. Dual Catalytic Activity of a Cytochrome P450 Controls Bifurcation at a Metabolic Branch Point of Alkaloid Biosynthesis in Rauwolfia serpentina. *Angew. Chem., Int. Ed. Engl.* **2017**, *56* (32), 9440−9444.

(22) Dang, T. T.; Franke, J.; Carqueijeiro, I. S. T.; Langley, C.; Courdavault, V.; O'Connor, S. E. Sarpagan bridge enzyme has substrate-controlled cyclization and aromatization modes. *Nat. Chem. Biol.* **2018**, *14* (8), 760−763.

(23) Payne, R. M.; Xu, D.; Foureau, E.; Teto Carqueijeiro, M. I.; Oudin, A.; Bernonville, T. D.; Novak, V.; Burow, M.; Olsen, C. E.; Jones, D. M.; Tatsis, E. C.; Pendle, A.; Ann Halkier, B.; Geu-Flores, F.; Courdavault, V.; Nour-Eldin, H. H.; O'Connor, S. E. An NPF transporter exports a central monoterpene indole alkaloid intermediate from the vacuole. *Nat. Plants* **2017**, *3*, 16208.

(24) Pompon, D.; Louerat, B.; Bronine, A.; Urban, P. Yeast expression of animal and plant P450s in optimized redox environments. *Methods Enzymol* **1996**, *272*, 51−64.
(25) Schopfer, C. R.; Ebel, J. Identification of elicitor-induced cytochrome P450s of soybean (Glycine max L.) using differential display of mRNA. *Mol. Gen Genet* **1998**, *258* (4), 315−22.
(26) Schmidt, W.; Peters, S.; Beerhues, L. Xanthone 6-hydroxylase from cell cultures of Centaurium erythraea RAFN and Hypericum androsaemium L. *Phytochemistry* **2000**, *53* (4), 427−31.
(27) Webb, B.; Sali, A. Comparative Protein Structure Modeling Using MODELLER. *Curr. Protoc Bioinformatics* **2016**, *54*, 5.6.1−5.6.37.
(28) Zheng, W.; Zhang, C.; Li, Y.; Pearce, R.; Bell, E. W.; Zhang, Y. Folding non-homologous proteins by coupling deep-learning contact maps with I-TASSER assembly simulations. *Cell Rep. Methods* **2021**, *1* (3), 100014.
(29) Kelley, L. A.; Mezulis, S.; Yates, C. M.; Wass, M. N.; Sternberg, M. J. The Phyre2 web portal for protein modeling, prediction and analysis. *Nat. Protoc* **2015**, *10* (6), 845−58.
(30) Cramer, P. AlphaFold2 and the future of structural biology. *Nat. Struct Mol. Biol.* **2021**, *28* (9), 704−705.
(31) Trott, O.; Olson, A. J. AutoDock Vina: improving the speed and accuracy of docking with a new scoring function, efficient optimization, and multithreading. *J. Comput. Chem.* **2010**, *31* (2), 455−461.
(32) Gotoh, O. Substrate recognition sites in cytochrome P450 family 2 (CYP2) proteins inferred from comparative analyses of amino acid and coding nucleotide sequences. *J. Biol. Chem.* **1992**, *267* (1), 83−90.
(33) Seifert, A.; Pleiss, J. Identification of selectivity-determining residues in cytochrome P450 monooxygenases: A systematic analysis of the substrate recognition site 5. *Proteins: Struct., Funct., Bioinf.* **2009**, *74* (4), 1028−1035.
(34) Gricman, Ł.; Vogel, C.; Pleiss, J. Identification of universal selectivity-determining positions in cytochrome P450 monooxygenases by systematic sequence-based literature mining. *Proteins: Struct., Funct., Bioinf.* **2015**, *83* (9), 1593−1603.
(35) Munro, A. W.; Girvan, H. M.; Mason, A. E.; Dunford, A. J.; McLean, K. J. What makes a P450 tick? *Trends Biochem. Sci.* **2013**, *38* (3), 140−150.

https://doi.org/10.1021/acscatal.2c03405
ACS Catal. 2022, 12, 13630−13637